https://doi.org/10.3311/PPci.23308

Periodica Polytechnica Civil Engineering, 68(3), pp. 859–871, 2024

Study on a 3D Train-Track-Bridge System Dynamic Behavior Subjected to Over-Height Collision Force

Amirhesam Taghipour[1], Jabbar Ali Zakeri[1*], Meysam Jahangiri[2], Seyed Ali Mosayebi[1]

[1] School of Railway Engineering, Iran University of Science and Technology, Hengam St., Resalat Square, 1684613114 Tehran, Iran
[2] Department of Civil Engineering and Transportation, University of Isfahan, Azadi square, 81746-73441 Isfahan, Iran
[*] Corresponding author, e-mail: zakeri@iust.ac.ir

Received: 28 August 2023, Accepted: 17 February 2024, Published online: 18 April 2024

Abstract

Railway bridges are built to allow trains to cross over highways, valleys, or other transportation infrastructure. In recent years, the number of railway bridges subjected to over-height collision forces has increased. These collisions damage the bridge and affect the safety of the running train. In this investigation, first, a 3D GT26 train-track-bridge interaction model was created to study the effects of collision forces applied to the bridge superstructure and not to the bridge piers as a novelty of this research using the finite element analysis. Then, the dynamic responses of the railway bridge due to the GT26 train load and subjected to over-height collision forces were obtained. Finally, the different sensitivity analyses describe that changing the length of the collision area, the bridge span, and the value of collision forces affect the dynamic responses of the bridge in the contact area. The results show that maximum lateral displacement of the concrete girder in case of assuming the GT26 train 3D model plus over-height collision force is 8.88% less than the case in which considering only freight train axle-load and same over-height collision force apply to the bridge superstructure, and its value reduces from 45 mm to 41 mm. The maximum lateral displacement of the bridge deck is reduced by about 71% by increasing the collision area length from 0.2 m to 1.2 m and at the impact area rises about 43.5% by changing collision speed from 48 km/hr to 144 km/hr as collision force from 7753 kN to 13370 kN.

Keywords

railway bridge, over-height collision force, train-track-bridge interaction model, finite element analysis

1 Introduction

The railway tracks are exposed to an ever-increasing demand for axial load and operation speed. To fulfill such requests the railway infrastructures also must satisfy the new requirements. In this consideration, the constructed bridges play an important role such that any flaw in the performance of the railway bridges interrupts the performance of the entire path. There are some studies that focus on the train–bridge interaction system and also its behavior under collision loads to the bridge piers. However, up to now, only a few papers have been published on the vibration of the train–bridge system induced by an over-height collision force to the bridge superstructure and its influence on the dynamic responses of the railway bridge system [1]. The dynamic behavior of a train-bridge interaction system is a complicated problem that involves vehicle (train) modelling and bridge system modelling issues [2, 3]. The dynamic response of the railway bridge-train interaction has been studied extensively [4–7]. For example, Cheng et al. [8] has considered on a 2D system with a layered track to obtain the dynamic response of the railway bridge. Cantero et al. [9] considered a finite element (FE) planar model that contains the behavior of the train, ballasted track, and bridge together. In this research, the train is represented as a combination of lumped masses, rigid bars, springs, and dashpots. Also, the track is modelled as a beam resting on periodically spaced sprung mass systems representing railway track components like pads, sleepers, ballast, and sub-ballast placed on a bridge. Kim et al. [10] created a detailed dynamic model of the train-bridge coupled system based on the modal superposition approach and investigated its dynamic features while the train is standing still or moving at low speeds. Ferreira and López-Pita [11] concentrated on a numerical model created to accurately forecast train-track dynamic interaction response not only instantaneously but also in a long-term viewpoint.

Cite this article as: Taghipour, A., Zakeri, J. A., Jahangiri, M., Mosayebi, S. A. "Study on a 3D Train-Track-Bridge System Dynamic Behavior Subjected to Over-Height Collision Force", Periodica Polytechnica Civil Engineering, 68(3), pp. 859–871, 2024. https://doi.org/10.3311/PPci.23308

The occurrence of accidental collisions between over-height vehicles and bridge superstructures in current years has commonly affected the safety of various bridge types and traffic systems in urban areas. For example, 61% of interchange bridges have been damaged due to over-height collision forces in the United States and such systems include about 14% of whole bridge damages [12]. The mechanism and reasons for an over-height vehicle-bridge collision are complicated due to intricate dynamic effects, variability in forces, and different types of bridge structural and geometry [13]. The collision between an over-height truck and a prestressed concrete box girder bridge was studied based on the finite element-based software by Kong et al. in 2020. In this article, the damage to the impacted girder and the collision force are analyzed. Then, sensitivity analysis was conducted to evaluate the effects of different parameters on peak force, average force, duration time, and impact impulse that later can be used in the study of the anti-collision design of the bridge [14].

The impact force of the vehicle using a real-vehicle collision test concerning the vehicle impacting diagonally against a vertical rigid wall was calculated successfully by Beason et al. [15]. In this study, based on the maximum impact load obtained from the above experiments, the first edition of the AASHTO [16] code was formed to specify the equal static force for the bridge pier design against vehicle collision [17]. Qiao et al. [18] placing an I-Lam panel made of a composite sandwich structure at the bottom or edge of concrete bridge girders offered a protective system for bridge superstructures and confirmed the significance of the maximum displacement and the extreme contact force in the design of this protective mechanism through finite element simulation and predictive investigation. Demartino et al. [19] developed a new method to apply lateral impact loads to reinforced concrete vertical components at the standard vehicular impact location. The experimental system involved two parts, the horizontal impact facility and the vertical drop hammer installation. The vehicle test was accelerated to move on the horizontal guide rails through the impact force of the drop hammer facility and the results of the piezoelectric sensor in front of the vehicle were calculated to investigate the time history of the impact load.

Taghipour et al. [20] investigated the dynamic behavior of the railway bridge duo to the over-height vehicle collision subjected to the bridge superstructure. In this study, different types of collision forces were considered by using a finite element model of a concrete girder railway bridge and simulation was done. Then, the sensitivity analyses performed on the effect of the presence and absence of train axle load at the same time by applying collision load to the bridge superstructure in bridge girder lateral displacement, also on the result of changing the bridge span length and the value and velocity of the impacting object on the bridge dynamic responses. In the present research, the dynamic behavior of a railway bridge subjected to 3D Train Load and over-height collision force is investigated. In this study, first, a 3D GT26 train- bridge interaction model to study the effects of collision forces applied to the bridge superstructure and not to the bridge piers due to the over-height vehicle is created using the finite element analysis. Then, the dynamic responses of the railway bridge system due to the GT26 train load and subjected to over-height collision forces will obtain. Finally, different sensitivity analyses such as changing the bridge span length, value of collision forces, and length of collision area will be performed in the contact area of over-height collision force and bridge girder. Fig. 1 shows the process of present research approach.

2 3D GT26 Train-Bridge model

In this section, first, the railway bridge model will be described then the details related to the GT 26 train model and also load conditions of the system will be prescribed. Finally, the 3D model of the railway bridge on which the GT 26 train is placed, including the impact of the collision force on the bridge superstructure, will present. The equations of motion for the train–bridge interaction system subjected to over-height collision force can be defined as:

$$\begin{bmatrix} m_{TT} & 0 \\ 0 & m_{BB} \end{bmatrix} \begin{Bmatrix} \ddot{Z}_T \\ \ddot{Z}_B \end{Bmatrix} + \begin{bmatrix} c_{TT} & c_{TB} \\ c_{BT} & c_{BB} \end{bmatrix} \begin{Bmatrix} \dot{Z}_T \\ \dot{Z}_B \end{Bmatrix} + \begin{bmatrix} k_{TT} & k_{TB} \\ k_{BT} & k_{BB} \end{bmatrix} \begin{Bmatrix} Z_T \\ Z_B \end{Bmatrix} = \begin{Bmatrix} P_{TB} \\ P_{BT} \end{Bmatrix} + \begin{Bmatrix} 0 \\ P_{collision} \end{Bmatrix} \tag{1}$$

In Eq. (1), where m, c, and k are mass, damping, and stiffness matrices of the train-bridge interaction system, $\boldsymbol{Z}$, $\dot{\boldsymbol{Z}}$ and $\ddot{\boldsymbol{Z}}$ are displacement, velocity, and acceleration vectors, respectively; P_{TB}, P_{BT} and $P_{\text{collision}}$ are interaction forces between Train and bridge also over-height collision force and the subscripts T and B illustrate moving train and railway bridge, respectively.

2.1 Bridge model

The single-span bridge is modeled as the concrete deck on the longitudinal concrete girders in this research. Also, the finite element method is used in dynamic bridge analysis, and collision loads are in the form of force time history,

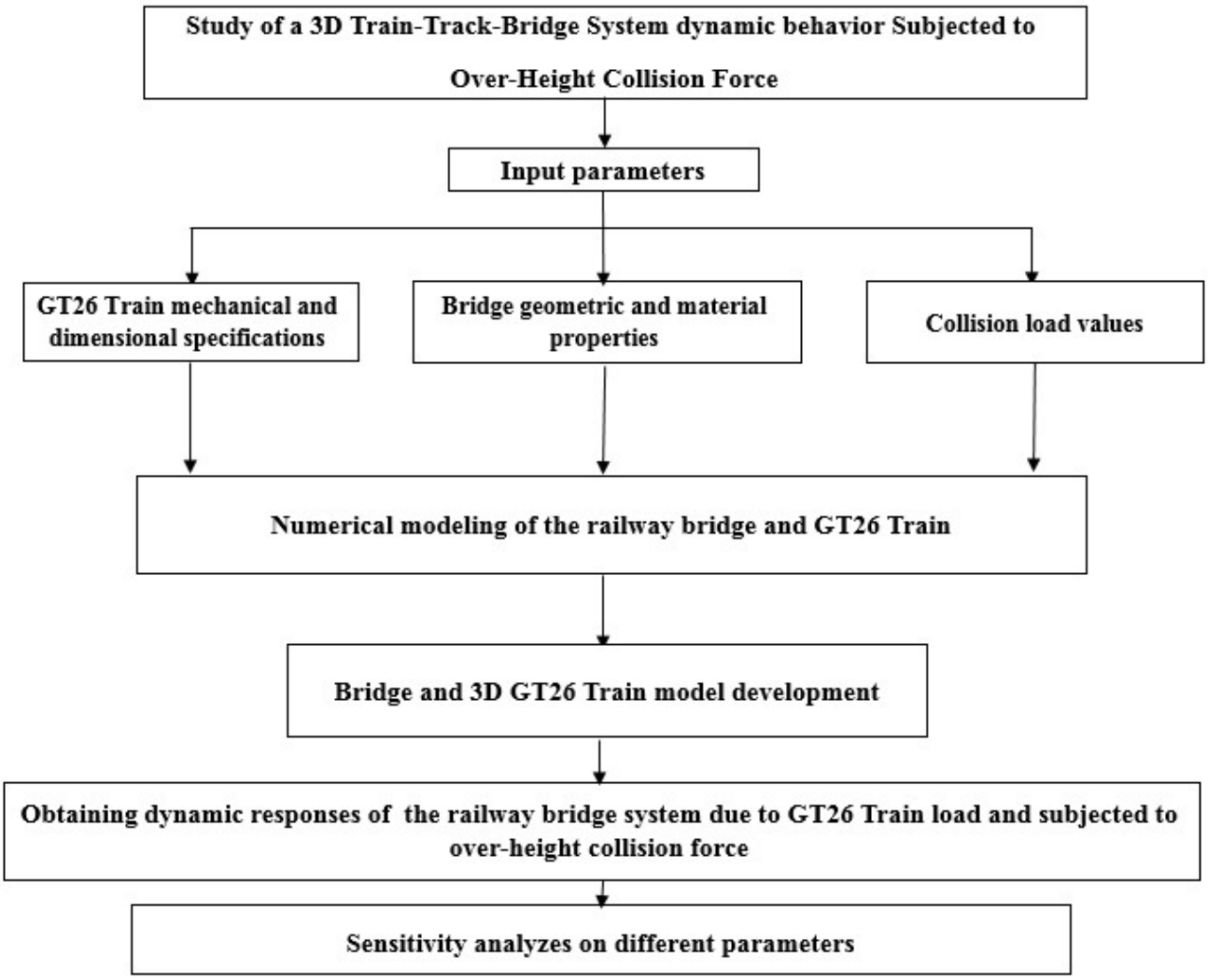

Fig. 1 The approach of the present research

applied to bridge superstructure, especially concrete girders. The model assumed to investigate the effect of an over-height collision force on the bridge superstructure is created by ABAQUS simulation software. In the mentioned model, the bridge superstructure is a concrete deck bridge with dimension values considered for its length, width, and slab thickness of 31 m, 7 m, and 0.3 m following AASHTO codes and leaflets related to railway bridge design. (AASHTO [16], Leaflets No. 301 [21], No. 139 [22], No. 139 [23]) In this paper, discrete rigid elements have been used instead of the bridge piers and abutments because a dead load of the bridge superstructure is so high that the limited weight of the passing train on the vertical deformations of the piers and abutments can be neglected. This is done to reduce the cost of the software analysis. The railway track model is a single-line ballasted track in this simulation. The specifications of the ballast mass have been selected by leaflet 301 (Technical and General Specification of the Ballasted Railway). The ballast is a hexahedral element, and each node has 6 degrees of freedom. The kind of sleeper used in the model is named B70, and the rail profile also has the mechanical and geometric specifications of the UIC 60 rail profile. In this simulation, rail takes place 5 cm above the sleepers due to the stiffness and damping of the rail pad and fastener such as spring and dashpot connections. Also, neoprene placed at a spacing of 20 cm from the outer side of the concrete girder is at the connection point to the rigid plates. Regarding the boundary conditions applied to the bridge model, the transitional and rotational degrees of freedom of the girders and rigid plates in the bridge model and the transitional degrees of freedom at both ends of the rails in the

railway track model are fixed in vertical, horizontal and lateral directions. Table 1 shows the geometric characteristics and types of materials for railway bridges [24]. Fig. 2 shows the 3D view of concrete girder railway bridge.

2.2 GT26 train model

In this research, GT26 train specifications have been used for modeling a vehicle on the railway bridge and all translational and rotational degrees of freedom have been considered in the form of a car body with a two-axle bogie with 27 degrees of freedom. Also the car body, bogies, and wheel axles are modeled as a rigid body with rotational inertia and were connected by springs and dashpots to each other. Regarding the boundary conditions applied to the GT26 train FE model, the transitional degrees of freedom of the train car body, bogie and wheel axle are fixed in a horizontal direction. Additionally, the rotational degrees of freedom on the wheel axles are restricted in both vertical and horizontal directions. Table 2 provides the geometric properties used in the finite element model of a GT26 train [20, 25–27]. Fig. 3(a) to 3(b) and Fig. 4(a) to 4(b) also represents the finite element simulation of GT26 train car body, bogie, wheel-axle and part of a wheel section by ABAQUS software respectively.

In this article, at the GT26 train for connecting the car body to the bogie at the secondary suspension system and for connecting the bogie to the wheel axles at the primary

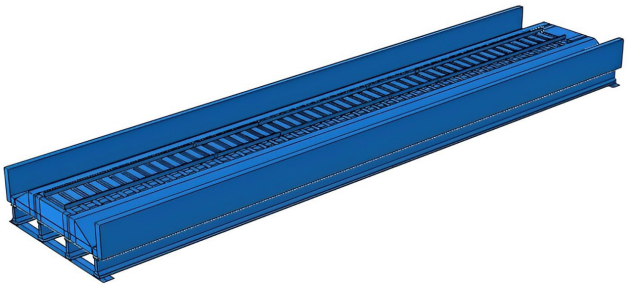

Fig. 2 The 3D view of concrete girder railway bridge [20] (Scale: 3 to 10000)

Table 1 Geometric characteristics and type of materials used in the finite element model of a railway bridge [20]

Parameter	Value	Unit
E_R	200	GPa
L_R	29.64	m
W_{RP}	60	mm
H_{RP}	180	mm
I_{RP}	30 550 000	mm^4
D_R	7 850	kg/m^3
E_S	26	MPa
L_S	2 600	mm
W_S	220	mm
H_S	230	mm
H_B	75	cm
D_B	1 400	kg/m^3
ϑ_B	0.25	-
K_{vrp}	240 000	kN/m
K_{lf}	24 000	kN/m
C_{vrp}	248	kN.s/m
C_{lf}	248	kN.s/m
K_{vn}	4 826 430	kN/m
K_{ln}	5 560	kN/m
H_n	171	mm

Table 2 Geometrical properties used in the finite element model of a GT26 Train [20, 25–27]

Parameter	Value	Unit
L_C	15.06	m
W_C	2.095	m
M_C	59	ton
I_{cx}	85	ton.m^2
I_{cy}	2 900	ton.m^2
I_{cz}	2 870	ton.m^2
L_b	4.2	m
W_b	2.095	m
H_b	1.15	m
M_b	3	ton
I_{bx}	1.55	ton.m^2
I_{by}	2.4	ton.m^2
I_{bz}	2.6	ton.m^2
L_{ws}	1.795	m
W_{ws}	0.1	m
H_{ws}	0.4	m
M_{ws}	1.8	ton
I_{wx}	2.1	ton.m^2
I_{wy}	2.1	ton.m^2
I_{wz}	0.043	ton.m^2
$L_{wheel\ section}$	70	mm
$W_{wheel\ section}$	94.205	mm
$H_{wheel\ section}$	150	mm
$D_{wheel\ section}$	7 850	kg/m^3

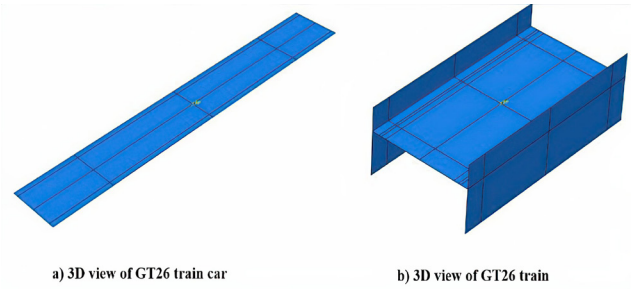

Fig. 3 The FE simulation of train GT26 car body and Bogie (Scales: a) 6 to 10000, b) 2 to 10000)

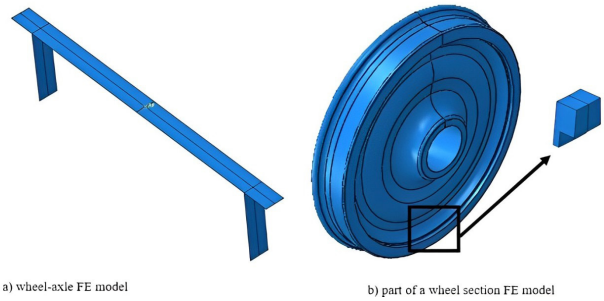

Fig. 4 The GT26 train wheel-axle and part of a wheel section model (Scales: a) 5 to 1000, b) 1 to 100)

suspension system springs and dashpots are considered in both vertical and horizontal directions. The wheel axles are also connected to the small section of the wheel on top of the rail due to the Hertzian spring to perform the simulation process more precisely and accurately according to Eq. (2) [27]:

$$K_H = \sqrt[3]{\frac{6G^2 Q_0 L_e}{(1-\nu)^2}} \tag{2}$$

In Eq. (2) K_H is the equivalent stiffness of Hertzian spring, Q_0 is contact force, L_e is equivalent wheel radius, G is shear modulus, and ϑ is Poisson's ratio. Table 3. identifies the mechanical specifications for spring and dashpot values used in the FE simulation Process. Also, Fig. 5 expresses the side view and section view of the GT26 train, including springs and dashpots between different parts of the vehicle.

The loading pattern of collision force because of concrete conduit pipe as a impacting object applied to the railway bridge superstructure in the middle of the concrete girder and at the connection point of the girder web and bottom flange including the GT26 train load is a triangular dynamic load with a value of 8653 kN and time domain of 3ms according to the studies conducted by Oppong et al. [28] and Taghipour et al. [20]. The mass of each part of the car body, bogie, and wheel axle is also applied to the system as a downward gravity force using the data in Table 2. Fig. 6 shows the general form of the GT26 train load and lateral collision force on the superstructure of the railway bridge. Fig. 7 depicts the section view of the 3D GT 26 train-railway bridge including spring and dashpots between different components of the system.

Table 3 Mechanical specifications used in the finite element model of a GT26 train [20, 25–27]

Parameter	Value	Unit
K_{vps}	970	kN/m
K_{lps}	2 350	kN/m
C_{vps}	25	kN.s/m
C_{lps}	62	kN.s/m
K_{vss}	810	kN/m
K_{lss}	105	kN/m
C_{vss}	45	kN.s/m
C_{lss}	40	kN.s/m
K_H	1.4×10^9	N/m

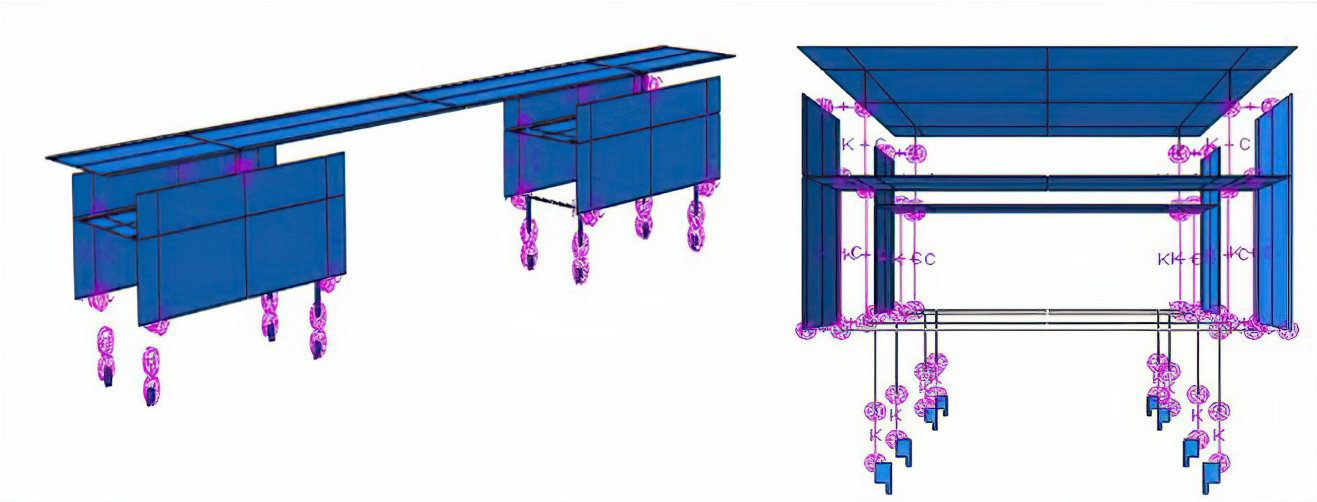

Fig. 5 The side view and section view of GT26 train including spring and dashpots between different parts of the vehicle (Scale: 6 to 10000)

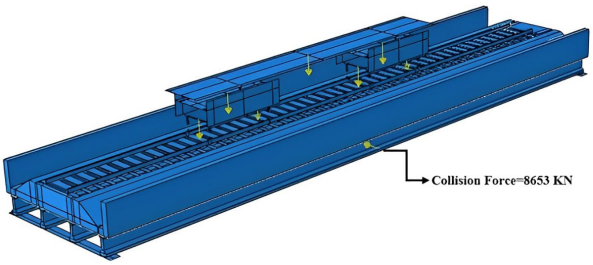

Fig. 6 General form of the 3D GT 26 train-railway bridge loading model (Scale: 3 to 10000)

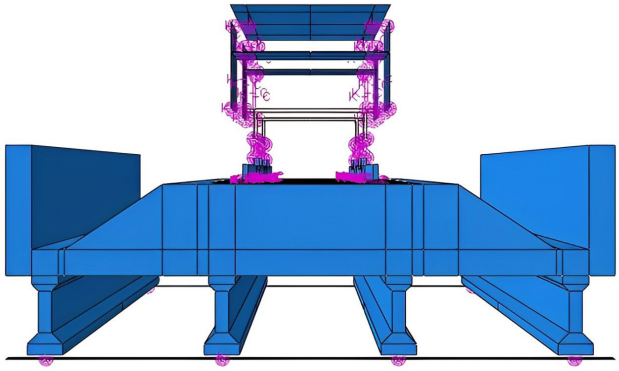

Fig. 7 The section view of the 3D GT 26 train-railway bridge including spring and dashpots between different components of the system

Fig. 8(a) shows a 3D GT26 train-railway bridge finite element model, and Fig. 8(b) also describes its mesh model. Among various mesh sizes such as 0.3, 0.25, 0.2, 0.15 for different elements of the railway bridge and GT26 train due to the lack of change in dynamic responses of the whole system, such as lateral displacement and acceleration at the bottom of the concrete girder to change the mesh size from 0.2 to 0.15 and from 0.15 to 0.1, the mesh size 0.2 had preferred.

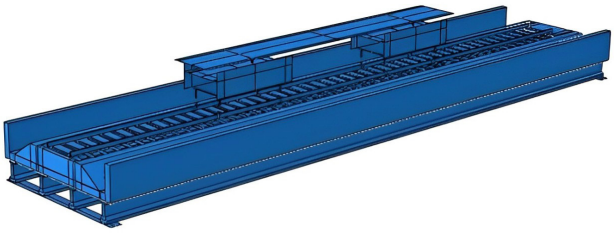

a) The whole model of 3D GT26 train and railway bridge

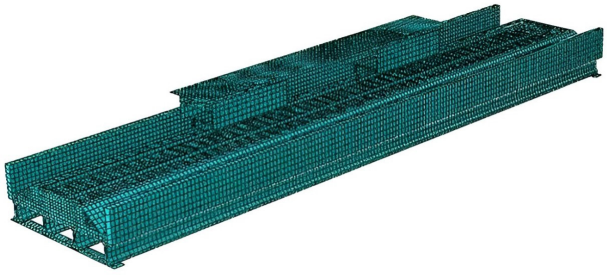

b) The mesh model of 3D GT26 train and railway bridge

Fig. 8 The 3D GT26 train-railway bridge finite element and mesh model (Scale: 3 to 10000)

2.3 Model validation

The results of experimental tests and numerical simulations according to the studies of Taghipour et al. [20], Oppong et al. [28], Saini and Shafei [29–32] for investigating the effect of over-height collision force on the bridge superstructure have been used for the model validation in this research. A repetition of the validation cases conducted in the mentioned studies has been avoided since the same validated models have been used in the current investigation. Further information is the output of dynamic responses in this article had a good correlation in comparison with the dynamic responses of the railway bridge-train system in Taghipour et al.'s research in 2023 for the same collision load applied to the railway bridge. Also, the difference as a result of the investigations carried out in the validation process of the model with the results of the field experiments and numerical simulations of Oppong et al. study in 2021 for two different collision loads of 8700 kN and 11500 kN is less than 0.5% and 4%, respectively.

3 Dynamic responses of the railway bridge system due to the GT26 train load and subjected to over-height collision force

In this study, the dynamic responses of the different components of the railway bridge, such as the concrete girder and the rail subjected to the over-height collision force and the GT 26 train load, are investigated. The results be shown in Fig. 9(a) to 9(b) are related to the rail lateral acceleration and bridge concrete girder lateral displacement in the middle of the railway bridge span respectively. The values of over-height collision force due to the concrete conduit pipe as an impacting object to the bridge superstructure and collision duration time are 8653 kN and T = 3 ms respectively based on the authors last research that cited here [20].

Fig. 9(a) shows the time history of rail acceleration during the collision period for the 8653 kN over-height collision force, including GT26 train load. Fig. 9(b) also shows the lateral displacement of a concrete girder for the 8653 kN collision load and the GT26 train load. The maximum lateral displacement values of the bottom of the concrete girder for the collision load of 8653 kN including GT26 train load is 0.04 m and the maximum lateral acceleration of top of the rail in the middle of the railway bridge span according to the Fig. 8(a) is 0.9 m/s^2.

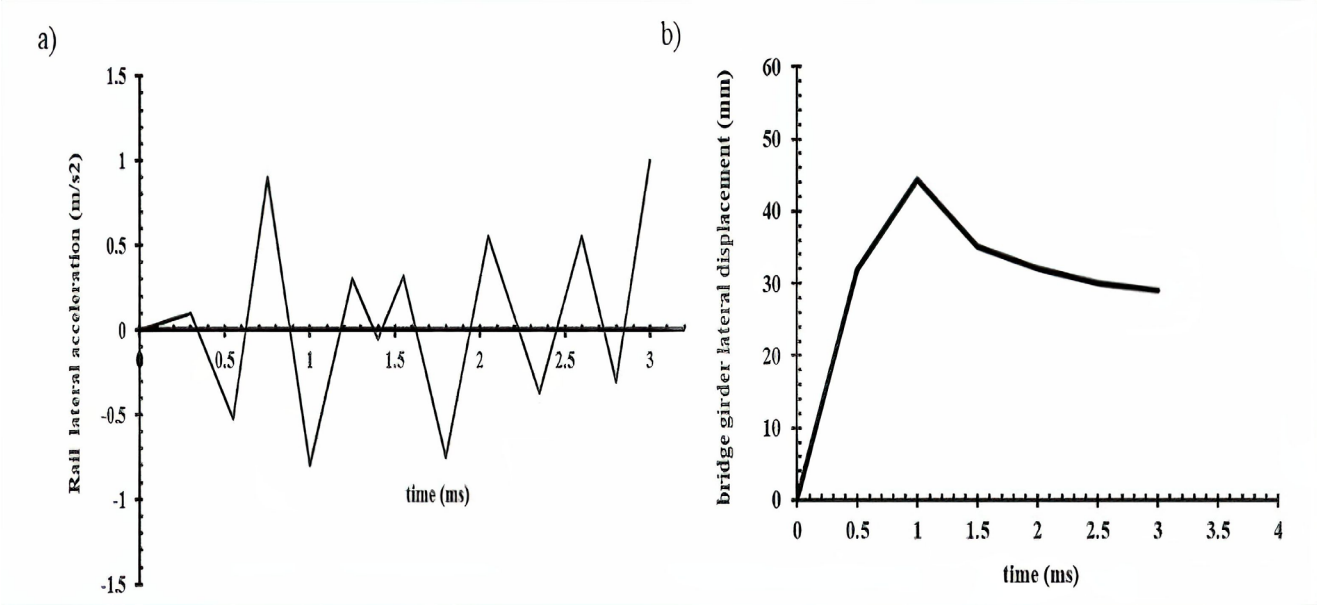

Fig. 9 The dynamic responses of the concrete girder and rail subjected to the GT26 train load and over-height collision force in the middle of the railway bridge span

4 Sensitivity analyses on different parameters

In this section, sensitivity analyses have been conducted on various parameters in the finite element model. The lateral displacement difference for the bridge girder including the GT26 train load and just the freight train axle load (25 tons) for the same over-height collision force in both cases is presented in Fig. 10.

As can be noticed from the graphs in Fig. 10, the lateral displacement values of the bridge girder bottom in the case of considering the GT26 train plus over-height collision force are more in comparison with a case of just applying freight train axle load plus the same over-height collision force in the first case. This gap of lateral displacement values for the concrete girder in the middle of the bridge span in the time range of 0.5 ms to1.5 ms is more evident due to the Fig. 10 diagrams. Fig. 11 displays the bridge deck lateral displacement subjected to the GT26 train load and over-height collision force in the middle of the railway bridge span for different collision area lengths.

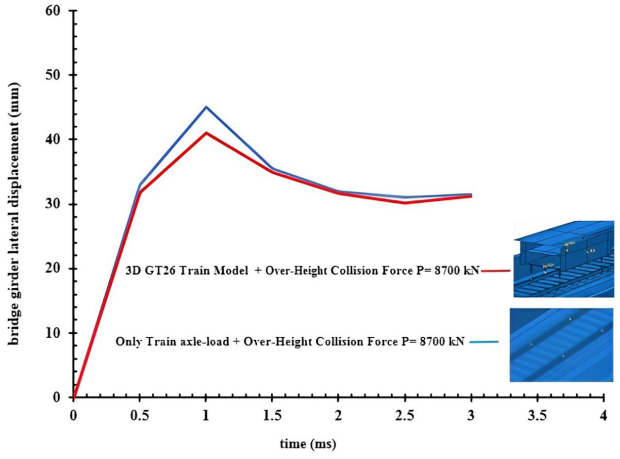

Fig. 10 The bridge girder lateral displacement difference subjected to the GT26 train load plus over-height collision force and just train axle-load plus over-height collision force in the middle of the railway bridge span.

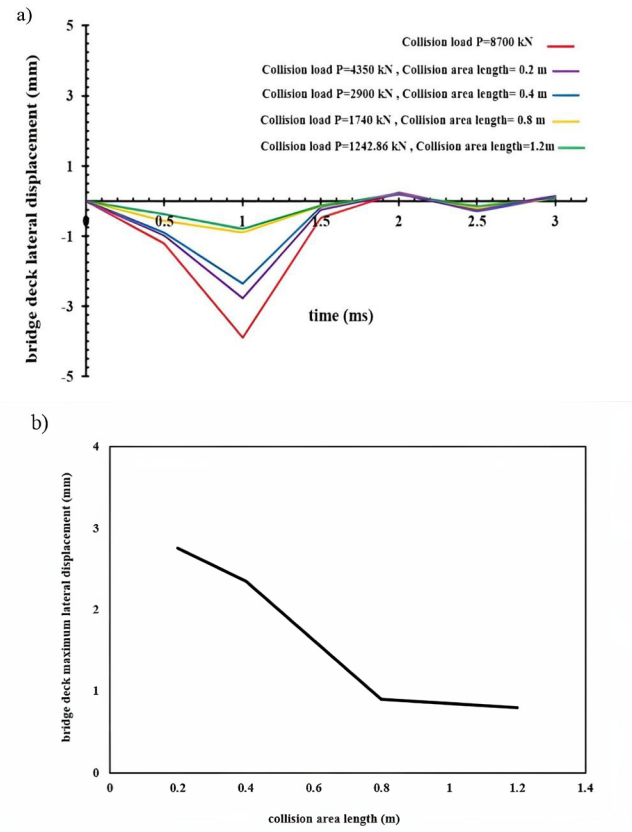

Fig. 11. a) The bridge deck lateral displacement and b) bridge deck peak lateral displacement subjected to the GT26 train load and over-height collision force in the middle of the railway bridge span for different collision area lengths.

It can be seen from Fig. 11(a) that the bridge deck lateral displacement values due to the GT26 train load and over-height collision force at the middle of the bridge span by increasing the collision area length and by moving away from the impact point as a result of the distribution of the primary collision force along the collision area length to the smaller values decrease. Also, Fig. 11(b) exhibits the graph of the maximum lateral displacement changes of the bridge deck for the different collision area lengths, such as 0.2, 0.4, 0.8, and 1.2 meters. The peak lateral displacement values for the collision area lengths 0.2 and 1.2 are 3.9 mm and 0.8 mm respectively. The results show that by increasing the length of the collision area from 0.2 to 1.2 m, the maximum lateral displacement was reduced by approximately 71%. Fig. 12(a) considers the effects of different bridge span lengths on the lateral displacement values of the railway bridge deck. Also, Fig. 12(b) exhibits the graph of the maximum lateral displacement changes of the bridge deck for the different bridge span lengths, like 25, 31 and 35 meters. In Fig. 12, the value of collision force and the GT26 train mechanical and geometrical specifications, also mechanical properties of the railway bridge construction materials like concrete modulus of elasticity, density, Poisson's ratio and ets., are assumed fixed.

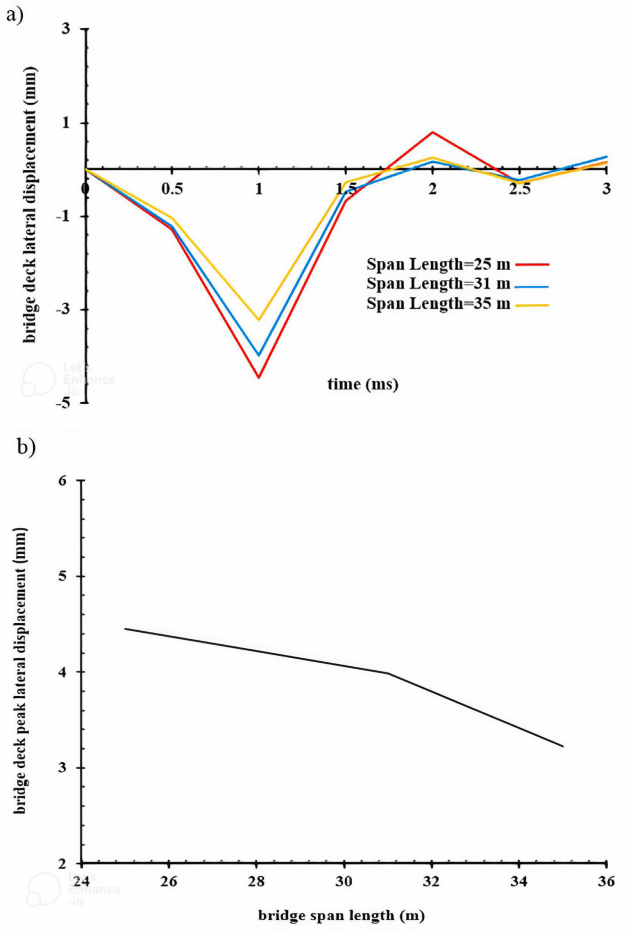

Fig. 12 a) The bridge deck lateral displacement and b) bridge deck peak lateral displacement subjected to the GT26 train load and over-height collision force in the middle of the railway bridge span for different bridge span lengths.

It can be seen from Figs. 12(a) and 12(b) that lateral displacements of the bridge deck in the middle of the railway bridge by increasing the bridge span length and weight decrease because by enhancing the inertial resistance of the bridge and moving away from the impact area due to the effects of geometric damping of the bridge, the intensity of these responses gradually reduce. The maximum lateral displacement values for the bridge span lengths 25 m and 31 m are 4.45 mm and 3.22 mm respectively. The results show that by increasing the bridge span length from 25 to 35 m, the maximum lateral displacement was reduced by approximately 27%. Fig. 13 and Fig. 14 also shows the effect of different types of collision load due to the different collision

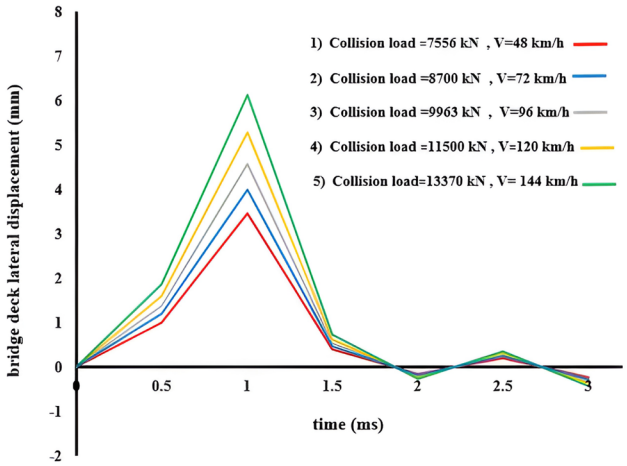

Fig. 13 The bridge deck lateral displacement subjected to the GT26 train load and over-height collision force in the middle of the railway bridge span for different collision loads due to the various collision speeds [20, 25, 26, 28].

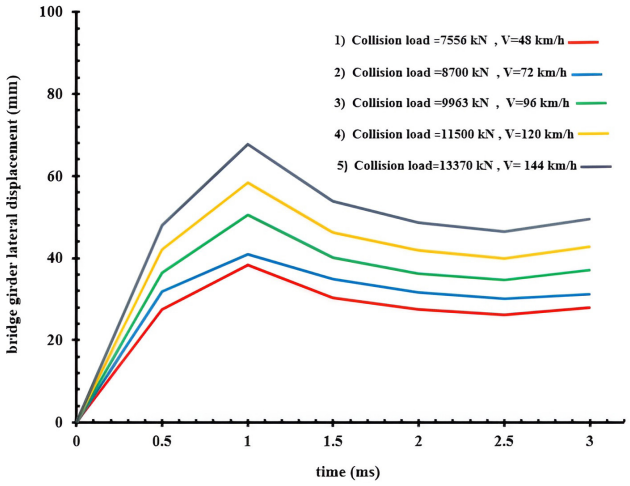

Fig. 14 The bridge girder lateral displacement in the middle of the railway bridge span for different collision loads due to the various collision speeds [20, 25, 26, 28].

speeds on the lateral displacement of the bridge deck and concrete girder in the middle of the railway bridge span respectively. The collision loads and related speeds took from the article by Oppong et al. [28] and Taghipour et al. [20, 25, 26] and calculated according to the Eq. (3):

$$P_{\text{collision}} = 79420\left(\frac{V}{S/q}\right)^{0.22} \times (R) \tag{3}$$

In Eq. (3), there is an exponential relationship between collision loads and speeds. Also, geometrical characteristics of the impacting object like the diameter (***S***: mm) and thickness of the impacting object (***q***: mm) and the contact area of the over-height vehicle collision (***R***: m^2) affected the collision speeds and loads [20–26].

In Fig. 13, by changing collision speed from 48 km/hr to 144 km/h, the collision load increases from 7753 kN to 13370 kN. As a result, the maximum lateral displacement in the impact area for the bridge deck enhances by about 43.48%. Also, the main change in the maximum lateral displacement occurs for the bridge deck in exchange for the collision force from 11500 kN to 13370 kN. In this case, the maximum lateral displacement increases by 13.98% and changes from 5.26 mm to 6.12 mm in the impact area. Fig. 14 shows the bridge girder lateral displacement subjected to the GT26 train load and over-height collision force in the middle of the railway bridge span for different collision loads due to the various collision speeds. Also, Fig. 15 depicts the correlation between maximum bridge girder lateral displacement and various collision speeds at the bottom of the concrete girder. According to Figs. 14 and 15 by changing collision speed from 48 km/h to 144 km/h, the collision load increases from 7753 kN to 13370 kN. As a result, the maximum lateral displacement in the impact area at the bottom of the bridge girder increases by about 43.5%. Also, the main change in the maximum lateral displacement occurs at the bottom of the concrete girder in exchange for the impact load from 11500 kN to 13370 kN. In this case, the maximum lateral displacement increases by 14% and changes from 0.05 m to 0.068 m in the impact area.

Fig. 16 displays the maximum lateral displacement values of the bridge deck subjected to the GT26 train load and over-height collision forces in the middle of the railway bridge for different span lengths. It can be seen that the maximum change for the lateral displacement values occurs for the span length of 25 m in the railway bridge for different collision loads. The slope of the lateral displacement diagram of the bridge deck for the 25 meter bridge span length for different collision speeds is 8.1% and 24.5% more than the 31 and 35 meter span lengths, respectively.

5 Results and discussion

The dynamic responses of the railway bridge including the GT26 train load for various over-height collision forces with different velocities for different bridge span lengths and also the effect of changing the collision area length at the connection point of the girder web to the bottom flange are discussed in this article. In the previous studies in collision areas, the effects of a collision load applied to the bridge piers were usually discussed but here in this work, the effects of over-height collision loads subjected to the bridge superstructure including 3D FE modeling of the GT26 train is considered a novelty of this research. The results show that the longer the collision area length,

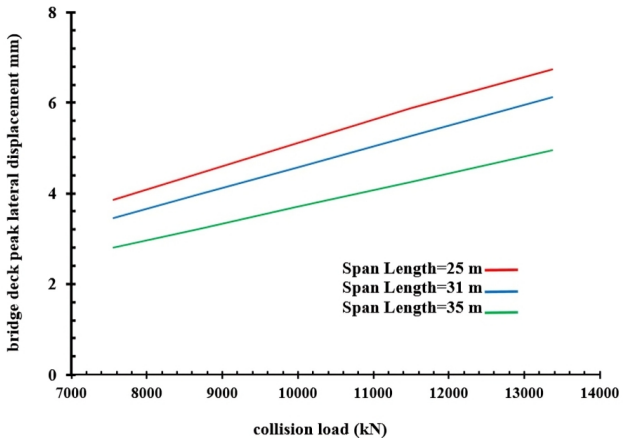

Fig. 15 The bridge girder lateral displacement subjected to the GT26 train load and over-height collision force in the middle of the railway bridge span for different collision loads due to the various collision speeds.

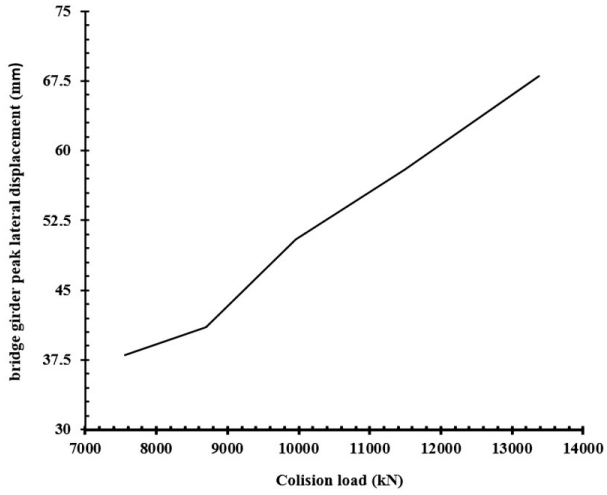

Fig. 16 The bridge girder lateral displacement subjected to the GT26 train load and over-height collision force in the middle of the railway bridge span for different collision loads due to the various bridge span lengths.

the smaller the lateral displacements of the bridge deck in the middle of the railway bridge span. Additionally, with the larger collision forces, the lateral displacement at the bridge girder and bridge deck increases, and longer bridge span lengths because of increasing in inertial resistance of the bridge lead to smaller lateral displacement values at bottom of the concrete girder and bridge deck. Some of the main results are summarized as follows:

- The maximum lateral acceleration of the rail subjected to the over-height collision force including the GT26 train load at the middle of the railway bridge span is 0.9 m/s^2 and the minimum value is 0.05 m/s^2.
- The maximum lateral displacement of the concrete girder in case of assuming the GT26 train 3D model plus over-height collision force is 8.88% less than the case in which considering only freight train axle-load and same over-height collision force apply to the bridge superstructure, and its value reduces from 45 mm to 41 mm at the collision area.
- The maximum lateral displacement of the bridge deck is reduced by about 71% by increasing the collision area length from 0.2 m to 1.2 m and reducing the over-height collision force from 4350 kN to 1243 kN at each point in collision area.
- The results show that minimum change in the maximum lateral displacement of the bridge deck occurs by adjusting the collision area length from 0.2 to 0.4 m by 14.8%.
- The maximum lateral displacement of the bridge deck is reduced by about 27.6% by increasing the bridge span length from 25 to 35 m.
- The results show that minimum change in the maximum lateral displacement of the bridge deck occurs by adjusting the span length from 31 to 35 meters by 19.13%.
- The maximum lateral displacement at the impact area at the bottom of the bridge girder due to over-height collision force including the GT26 train 3D model in the railway bridge rises about 43.5% by changing collision speed from 48 km/h to 144 km/h as collision force from 7753 kN to 13370 kN.
- The main change in the maximum lateral displacement happens when the collision load rises from 11500 kN to 13370 kN by 14% also in that case, lateral displacement increases from 0.0583 m to 0.0678m according to sensitivity analysis conducted at the bottom of the concrete girder.
- The maximum lateral displacement of the bridge deck at the impact area due to over-height collision force including the GT26 train 3D model in the railway bridge rises about 43.48% by changing collision speed from 48 km/h to 144 km/h as collision force increases from 7753 kN to 13370 kN.
- The main change in the maximum lateral displacement happens when the collision load rises from 11500 kN to 13370 kN by 14% also in that case, lateral displacement increases from 5.2 mm to 6.12 mm according to sensitivity analysis performed at the middle of railway bridge span for the bridge deck.
- The maximum lateral displacement of the bottom of the bridge concrete girder compared to the bridge deck due to over-height collision force, including the GT26 train 3D model at the middle of the bridge span, is rarely more by about 0.03%.
- The difference between the maximum lateral displacements of the bridge deck for minimum and maximum over-height collision forces due to the various impacting speeds for the 25 meter bridge span length is 2.8 mm.
- The difference between the maximum lateral displacements of the bridge deck for minimum and maximum over-height collision forces due to the various impacting speeds for the 31 meter and 35 meter bridge span lengths are 2.6 mm and 2.1 mm.
- The slope of the lateral displacement diagram of the bridge deck for the 25 meter bridge span length for different collision speeds is 8.1% and 24.5% more than the 31 and 35 meter span lengths, respectively.

Nomenclature

m_{TT} Train mass matrix [kg]
m_{BB} Bridge mass matrix [kg]
C_{TT} Train damping matrix [kN s/m]
C_{TB} Train-Bridge interaction damping matrix [kN s/m]
C_{BT} Bridge-Train interaction damping matrix [kN s/m]
C_{BB} Bridge damping matrix [kN s/m]
K_{TT} Train stiffness matrix [kN/m]
K_{BT} Train-Bridge interaction stiffness matrix [kN/m]
K_{BT} Bridge-Train interaction stiffness matrix [kN/m]
K_{BB} Bridge stiffness matrix [kN/m]
P_{TB} Train-Bridge interaction contact force [kN]
P_{BT} Bridge-Train interaction contact force [kN]

$P_{collision}$ Over-Height collision force [kN]
Q_0 Wheel-Rail contact force [kN]
K_H Equivalent stiffness of Hertzian spring [N/m]
G Wheel shear modulus of elasticity [N/m^2]
l_e Equivalent wheel radius [m]
ϑ Rail Poisson's ratio [-]
L_C Car body length [m]
W_C Car body width [m]
M_C Car body mass [kg]
I_{cx} Car body moment of inertia [ton.m^2]
I_{cy} Car body moment of inertia [ton.m^2]
I_{cz} Car body moment of inertia [ton.m^2]
I_{bx} Bogie moment of inertia [ton.m^2]
I_{by} Bogie moment of inertia [ton.m^2]
I_{bz} Bogie moment of inertia [ton.m^2]
I_{wx} Wheel-set moment of inertia [ton.m^2]
I_{wy} Wheel-set moment of inertia [ton.m^2]
I_{wz} Wheel-set moment of inertia [ton.m^2]
L_b Bogie length [m]
W_b Bogie width [m]
H_b Bogie Height [m]
M_b Bogie mass [kg]
L_{ws} Wheel-set length [m]
W_{ws} Wheel-set width [m]
H_{ws} Wheel-set height [m]
M_{ws} Wheel-set mass [kg]
$L_{wheel\ section}$ Section of a wheel length [m]
$W_{wheel\ section}$ Section of a wheel width [m]
$H_{wheel\ section}$ Section of a wheel height [m]
$D_{wheel\ section}$ Section of a wheel density [m]
E_R Rail modulus of elasticity [GPa]
L_R Rail length [m]
W_{RP} Rail profile width [mm]
H_{RP} Rail profile height [mm]
I_{RP} Rail profile moment of inertia [mm^4]
D_R Rail density [kg/m^3]
E_S Concrete sleeper modulus of elasticity [MPa]
L_S Sleeper length [mm]
W_S Sleeper width [mm]
H_S Sleeper height [mm]
H_B Ballast mass height [cm]
D_B Ballast density [kg/m^3]
ϑ_B Poisson's ratio of ballast material [-]
K_{vrp} Rail pad vertical stiffness [kN/m]
K_{lf} Fastener lateral stiffness [kN/m]
C_{vrp} Rail pad vertical damping [kN s/m]
C_{lf} Fastener lateral damping [kN s/m]
K_{vn} Neoprene vertical stiffness [kN/m]
K_{ln} Neoprene lateral stiffness [kN/m]
H_n Neoprene height [mm]
C_{lps} Primary system lateral damping [kN s/m]
K_{vss} Secondary system vertical stiffness [kN/m]
K_{lss} Secondary system lateral stiffness [kN/m]
C_{vss} Secondary system vertical damping [kN s/m]
C_{lss} Secondary system lateral damping [kN s/m]
K_{vps} Primary system vertical stiffness [kN/m]
K_{lps} Primary system lateral stiffness [kN/m]
C_{vps} Primary system vertical damping [kN s/m]
S Diameter of the impacting object [mm]
q Thickness of the impacting object [mm]
R Contact area of the over-height vehicle collision [m^2]

Funding Statement
The author(s) received no financial support for the research, authorship, and/or publication of this article.

Declaration of conflicting interest
The author(s) declared no potential conflicts of interest with respect to the research, authorship, and/or publication of this article.

References

[1] Xia, C. Y., Xia, H., Roeck, G. "Dynamic response of a train–bridge system under collision loads and running safety evaluation of high-speed trains", Journal of Composite Structures, 140, pp. 23–38, 2014. https://doi.org/10.1016/j.compstruc.2014.04.010

[2] Stefanidou, S. P., Paraskevopoulos, E. A. "Seismic fragility analysis of railway RC bridges considering real-time vehicle-bridge interaction with the aid of co-simulation techniques", Earthquake Engineering and Structural Dynamics, 51(9), pp. 2137–2161, 2022. https://doi.org/10.1002/eqe.3657

[3] Mosayebi, S. A., Zakeri, J. A., Esmaeili, M. "Investigations on Vehicle Interaction with CWR Tracks Considering Some Aspects of Rail Support Modulus", Periodica Polytechnica Civil Engineering, 62(2), pp. 444–450, 2018. https://doi.org/10.3311/PPci.10752

[4] Bucinskas, P., Andersen, L. V. "Dynamic response of vehicle–bridge–soil system using lumped-parameter models for structure–soil interaction", Computers & Structures, 238, 106270, 2020. https://doi.org/10.1016/j.compstruc.2020.106270

[5] Alkhdour, A., Tiutkin, O. L., Marochka, V. V., Boboshko, S. H. "The centrifugal modeling of reinforcement on approaches to railway bridges", Acta Polytechnica Hungarica, 19(3), pp. 131–142, 2022. https://doi.org/10.12700/APH.19.3.2022.3.11

[6] Harrach, D., Rad, M. M. "Comprehensive Laboratory Test Series for Timber-Concrete Composite Structures", Acta Polytechnica Hungarica, 20(1), pp. 231–250, 2023. https://doi.org/10.12700/APH.20.1.2023.20.16

[7] Harrach, D., Habashneh, M., Rad., M. M. "Numerical Investigation of Glue Laminated Timber Beams considering Reliability-based Design", Acta Polytechnica Hungarica, 20(1), pp. 109–122, 2023. https://doi.org/10.12700/APH.20.1.2023.20.8

[8] Cheng, Y. S., Au, F. T. K., Cheung, Y. K. "Vibration of railway bridges under a moving train by using bridge-track-vehicle element", Engineering Structures, 23(12), pp. 1597–1606, 2001. https://doi.org/10.1016/S0141-0296(01)00058-X

[9] Cantero, D., Arvidsson, T., O Brien, E., Karoumi, R. "Train–track–bridge modelling and review of parameters", Structure and Infrastructure Engineering, 12(9), pp. 1051–1064, 2016. https://doi.org/10.1080/15732479.2015.1076854

[10] Kim, K. J., Han, J. B., Han, H. S. "Coupled vibration analysis of maglev vehicle-guide way while standing still or moving at low speeds", Vehicle System Dynamics, 53(4), pp. 587–601, 2016. https://doi.org/10.1080/00423114.2015.1013039

[11] Ferreira, P. A., López-Pita, A. "Numerical modelling of high speed train/track system for the reduction of vibration levels and maintenance needs of railway tracks", Construction and Building Materials, 79, pp. 14–21, 2015. https://doi.org/10.1016/j.conbuildmat.2014.12.124

[12] Xu, L. J., Lu, X. Z., Smith, S. T., He, S. T. "Scaled model test for collision between over-height truck and bridge superstructure", International Journal of Impact Engineering, 49, pp. 31–42, 2012. https://doi.org/10.1016/j.ijimpeng.2012.05.003

[13] Das, S., Brenkus, N., Tatar, J. "Strategies for Prevention, Protection, and Repair of Bridge Girders Vulnerable to Over-height Vehicle Impacts: A State-of-the-Art Review", Journal of Structures, 44, pp. 514–533, 2022. https://doi.org/10.1016/j.istruc.2022.07.048

[14] Kong, L., Zhang, J., Han, W. "Investigation on Damage and Simplified Collision Force of Prestressed Concrete Box Bridge Subjected to Over-Height Truck Collision", International Conference on Intelligent Transportation, Big Data & Smart City (ICITBS), Vientiane, Laos, 2020, pp. 37–42. ISBN 9781728166995 https://doi.org/10.1109/ICITBS49701.2020.00016

[15] Beason, W. L., Hirsch, T. J., Campise, W. L. "Measurement of heavy vehicle impact forces and inertial properties", Texas Transportation Institute, Federal Highway Administration, Arlington, TX, USA, Report/Paper Numbers: FHWA/RD-89/120, RF-7046, 1989.

[16] AASHTO "AASHTO LRFD bridge design specifications", American Association of State Highway and Transportation Officials, 2017. ISBN 978-1-56051-654-5

[17] Xu, X., Zhang, H., Du, X., Liu, Q. "Vehicle collision with RC structures: A state-of-the-art review", Structures, 44, pp. 1617–1635, 2022. https://doi.org/10.1016/j.istruc.2022.08.107

[18] Qiao, P., Yang, M. S., Mosallam, A. "Impact analysis of I-Lam sandwich system for over-height collision protection of highway bridges", Engineering Structures, 26(7), pp. 1003–1012, 2004. https://doi.org/10.1016/j.engstruct.2004.03.004

[19] Demartino, C., Wu, J. G., Xiao, Y. "Response of shear-deficient reinforced circular RC columns under lateral impact loading", International Journal of Impact Engineering, 109, pp. 196–213, 2017. https://doi.org/10.1016/j.ijimpeng.2017.06.011

[20] Taghipour, A., Zakeri, J. A., Jahangiri, M., Mosayebi, S. A. "Investigating the dynamic behaviour of a railway bridge subjected to over-height vehicle collision", Australian Journal of Structural Engineering, 24(3), pp. 217–227, 2023. https://doi.org/10.1080/13287982.2023.2176972

[21] Iran Management and Planning Organization "Technical and General Specification of Ballasted Railway", Management and Planning Organization of Iran, Teheran, Iran, Leaflet. No. 301, 2006.

[22] Iran Management and Planning Organization "Technical and General Specification of highway and railway bridge design", Management and Planning Organization of Iran, Tehran, Iran, Leaflet. No. 139, 2001.

[23] Iran Management and Planning Organization "Technical and General Specification of reinforced concrete bridge design", Management and Planning Organization of Iran, Tehran, Iran, Leaflet. No. 395, 2009.

[24] Zhao C, Wang P, Xing M. "Research on the Matching of Fastener Stiffness Based on Wheel-Rail Contact Mechanism for Prevention of Rail Corrugation", Mathematical Problems in Engineering, 21, pp. 1–13, 2017. https://doi.org/10.1155/2017/6748160

[25] Taghipour, A., Zakeri, J. A., Mosayebi, S. A. "Investigations on the Effects of Rail Longitudinal Forces in Train-Track Dynamic Interaction", Periodica Polytechnica Civil Engineering, 68(2), pp. 364–374, 2023. https://doi.org/10.3311/PPci.22964

[26] Taghipour, A., Zakeri, J. A., Mosayebi, S. A. "Investigating the thermal force effect of the rail on dynamic analysis of railway track under dynamic load", Quarterly Journal of Transportation Engineering, 13(1), pp. 1149–1162, 2021. https://doi.org/10.22119/jte.2020.115215

[27] Sotoudeh, S., Jahangiri, M., Ranjbarnia, M., Zakeri, J. A. "Three-dimensional Modeling of an Old Masonry Bridge and Assessing Its Current Capacity", Periodica Polytechnica Civil Engineering, 64(2), pp. 460–473, 2020. https://doi.org/10.3311/PPci.14942

[28] Oppong, K., Saini, D., Shafei, B. "Characterization of impact-induced forces and damage to bridge superstructures due to over-height collision", Engineering Structures, 236, 112014, 2021. https://doi.org/10.1016/j.engstruct.2021.112014

[29] Saini, D., Shafei, B. "Performance of concrete-filled steel tube bridge columns subjected to vehicle collision", Journal of Bridge Engineering, 24(8), pp. 1–13, 2019. https://doi.org/10.1061/(ASCE)BE.1943-5592.0001439

[30] Saini, D., Shafei, B. "Investigation of concrete-filled steel tube beams strengthened with CFRP against impact loads", Journal of Composite Structures, 208, pp. 744–757, 2019.
https://doi.org/10.1016/j.compstruct.2018.09.057

[31] Saini, D., Shafei, B. "Concrete constitutive models for low velocity impact simulations", International Journal of Impact Engineering, 132, pp. 1–13, 2019.
https://doi.org/10.1016/j.ijimpeng.2019.103329

[32] Saini, D., Shafei, B. "Prediction of extent of damage to metal roof panels under hail impact", Engineering Structures, 187, pp. 362–371, 2019.
https://doi.org/10.1016/j.engstruct.2019.02.036